CHAPTER 5

Pool boiling characteristics of water on textured surfaces

The surface fabrication method and characteristics of various textured surfaces are already discussed in Chapter 3. In this chapter an effort has been made to study the effects of surface characteristics on pool boiling performance parameters such as boiling curve, onset of nucleate boiling (ONB), and heat transfer coefficients will be discussed for three different cases of surface as follows.

5.1. Pool boiling performance curve

A Series of experiments were conducted on twelve different surfaces (see section 3.2.1) to study the effects of composites, textured, and coating layer thickness on pool boiling performances. Surfaces are prepared by the electrophoretic deposition technique using three different hybrid nanofluids, by varying the coating duration which has already been discussed in Chapter 3 (section 3.1). All experiments were conducted in demineralised (Milli-Q) water at nearly saturation temperature (99.7±0.2°C) and atmospheric conditions. The supplied heat flux is varied in small steps to have more data and was restricted below the CHF to prevent the thermal damage of cartridge heater. The data obtained from the polished copper (bare) surface is used as reference data to compare the performance with the coated surface. The effect of different coating materials and coating duration on the pool boiling curve has been discussed in the following sections.

5.1.1. Effect of TiO_2-SiO_2 coating

Experiments were conducted on four different surfaces named CS1-5, CS1-10, CS1-15, and CS1-20. These surfaces were, made by varying the deposition time 5, 10, 15, and 20 minutes, respectively. **Fig. 5.1,** shows a boiling curve between the heat flux and wall superheat (ΔT) of coated and bare surfaces. From the boiling curve **(Fig. 5.1),** it is observed that the trend of the boiling curve is similar (convex upward) for the samples CS1-5, CS1-10, and CS1-15 below the partial nucleate boiling region ($q'' < 400$ kW/m^2) whereas different (convex downward) for sample CS1-20 and bare surface. As the coating duration increases from 5 to 10 and 15 minutes, the boiling curve becomes steeper and shifts to the left. Shifting of the boiling curve reflects that there is a reduction in wall temperature caused by increased heat dissipation from the surface.

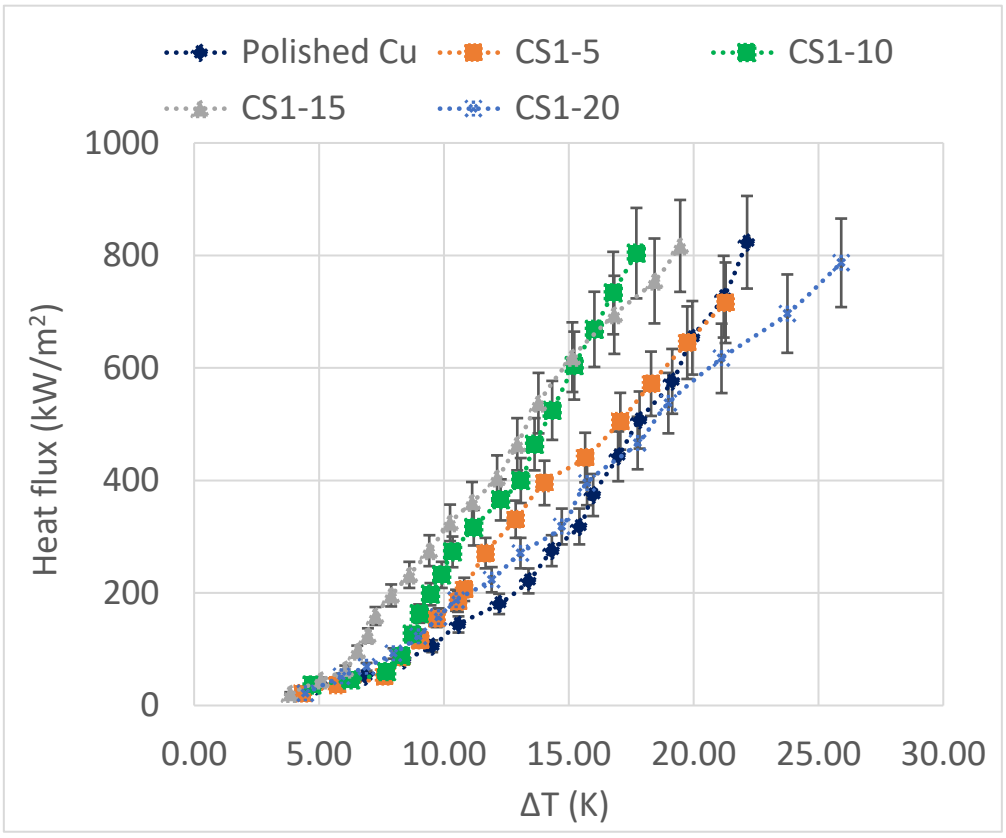

Fig. 5.1. Pool boiling performance curve of polished Cu and TiO_2-SiO_2 coated surface.

When the coating time further increased to 20 minutes, the boiling curve of sample CS1-20 started shifting towards the bare surface. In the case of CS1-5, CS1-10, and CS1-15 improved wettability, roughness, and surface morphology are responsible for the higher heat transfer and reduction in wall superheat. Whereas in later case comparatively dense and higher coating layer thickness acts as an insulating layer, and supress the wettability and roughness effects, resultant heat dissipation from the surface was affected and comparatively higher wall temperature was observed. However as supplied heat flux increased beyond 400 kW/m^2 its effects are more prominent where an increase in wall superheat is even higher than the on polished Cu at similar heat fluxes. Therefore, the effect of coating is beneficial when the coating layer thickness is maintained below ~10µm in this particular case, and beyond it, heat transfer starts deteriorating, due to an increase in thermal resistance as coast of higher coating layer thickness.

5.1.2. Effect of TiO_2 - Al_2O_3 coatings

Pool boiling experiments were performed on four different surfaces named CS2-2.5, CS2-5, CS2-10, and CS2-15, which were made by varying the coating duration 2.5, 5, 10, and 15 minutes, respectively (see section 3.2.1.2). Fig. 5.2 shows, the pool boiling performance curve of TiO_2 - Al_2O_3 coated surface. By looking at Fig. 5.2, it can be seen that the boiling curve trend for samples CS2-2.5, CS2-5, and CS2-10, are similar but shifted towards the left of the polished Cu surface. In the case of CS2-15, the curve initially follows the bare surface up to the heat flux of nearly 220 kW/m^2 then begins to shift towards the right and continues to do so until the maximum heat flux condition is reached.

These differences in boiling curves can be linked to the surface wettability and coating thickness of the sample. We have seen in Chapter 3 that as coating duration increases contact angle decreases, and coating thickness increases. Also, the bare surface is hydrophilic in nature, whereas coated surfaces are hydrophobic in nature. For a hydrophobic surface decrease

in contact angle means an increase in wettability. Fig. 5.2 also shows that, initially, up to the heat flux of 220 kW/m^2 the wall superheat of surface CS2-2.5 and CS2-5 are nearly same; beyond this, as heat flux increases, its difference starts growing, and a significant difference in the wall superheat is observed for the heat flux beyond 400 kW/m^2. In this case coating duration decreased below 5 minute to discover the optimum coating layer, as it can observed that boiling curve initially shifted to-wards the left for CS2-2.5, CS2-5, and then it shifted towards the right of the bare surface (CS2-10, and CS2-15) as shown in Fig. 5.2.

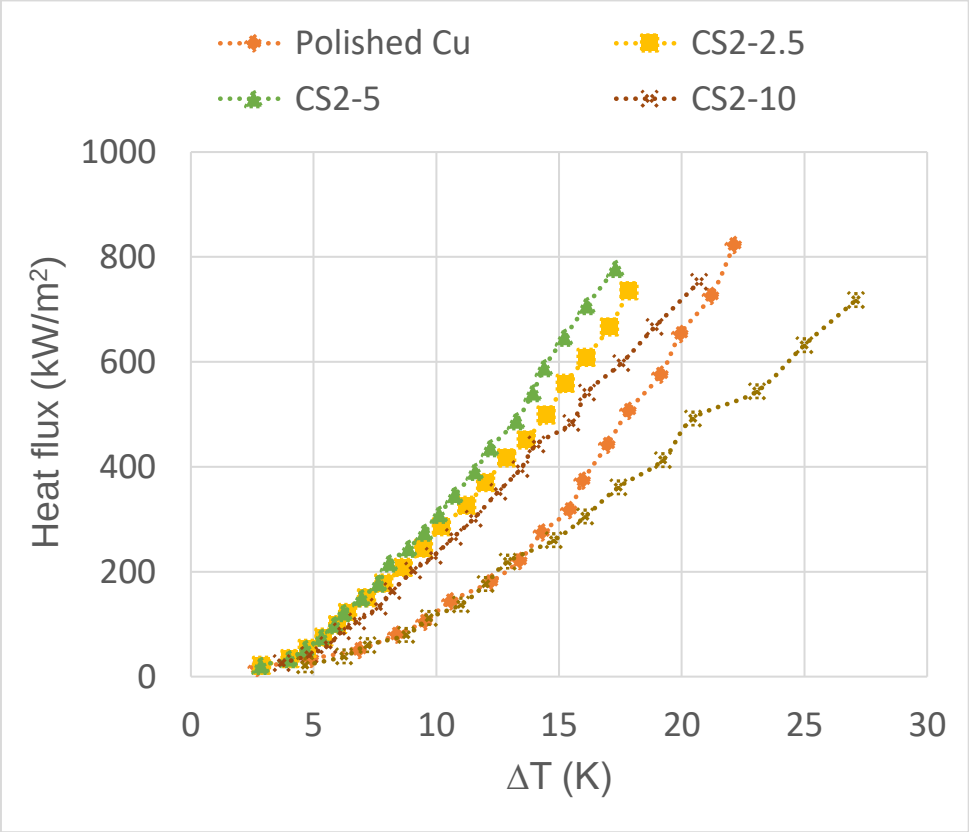

Fig. 5.2. Pool boiling performance curve of polished Cu and TiO_2 - Al_2O_3 coated surface.

This is because of the marginal increase in wettability, and roughness reduces the bubble elongation effect and helps in the early departure [124] and various dimple-like structure (Fig. 3.8 b), which may be activated and acts as nucleation sites. In the case of sample CS2-10, as the coating duration increased to 10 minutes, the dimple structure was omitted and a large number of thin partial cavity lines appeared on the surface (Fig. 3.8 c).

As the coating time further increased to 15 minutes, the thin partial cavity line grew and formed like a nano-channel structure (Fig. 3.8 d). The surfaces CS2-10, and CS2-15, have greater surface roughness and a lesser contact angle; despite these, the growth in wall superheat is even higher than the CS2-2.5 and CS2-5, specifically above the heat flux of 450 kW/m^2 and 250 kW/m^2, respectively. This may be because a significant increase in coating layer thickness the thermal resistance of the surface increased, due to which initial bubble formation, growth, and departure frequency of the surface [18-19, 83] were affected. Therefore, wall superheat grows faster as the coating layer thickness increases above ~15μm and its value is even greater than the bare surface in the case of sample CS2-15, where the coating layer thickness increased to ~ 38μm.

5.1.3. Effect of SiO_2 - Al_2O_3 coatings

Fig. 5.3, shows a pool boiling performance curve of SiO_2 - Al_2O_3 coated surfaces and compared with the polished copper. The samples CS3-5, CS3-10, CS3-15, and CS3-20, refer to the surface prepared by varying the coating duration 5, 10, 15, and 20 minutes in SiO_2 - Al_2O_3 hybrid nanofluids. It is observed that, the trend of the boiling curve is similar for the samples CS3-5, CS3-10, and CS3-15 whereas for the sample CS3-20 is different. Initially, as the coating duration increased from 5 to 15 minutes, corresponding to the boiling curve of the samples CS3-5, CS3-10, and CS-15 shifted left to the bare surface and became steeper. As coating time further increased to 20 minutes, the boiling curve started shifting towards the bare surface and later crossed it when the supplied heat flux reached beyond~ 480 kW/m^2. The change in surface characteristics such as surface morphology, wettability, and roughness may play a key role in lower wall superheat for the samples CS3-5, CS3-10, and CS3-15. Nevertheless, for the sample CS3-20, increased coating layer thickness plays a dominant role in poor heat dissipation and higher wall temperature. However, it has already been mentioned that the coated surfaces are hydrophobic in nature whereas polished Cu is hydrophilic in

nature. As the coating duration increases static contact angle increases which indicates wettability decreases. Earlier Bourdon et al. **[**125] also revealed that the surface with low wettability needed low wall superheat (ΔT) for bubble formation. Similarly, Jo et al. [126] observed that there was a decrease in wall superheat with a decrease in surface wettability.

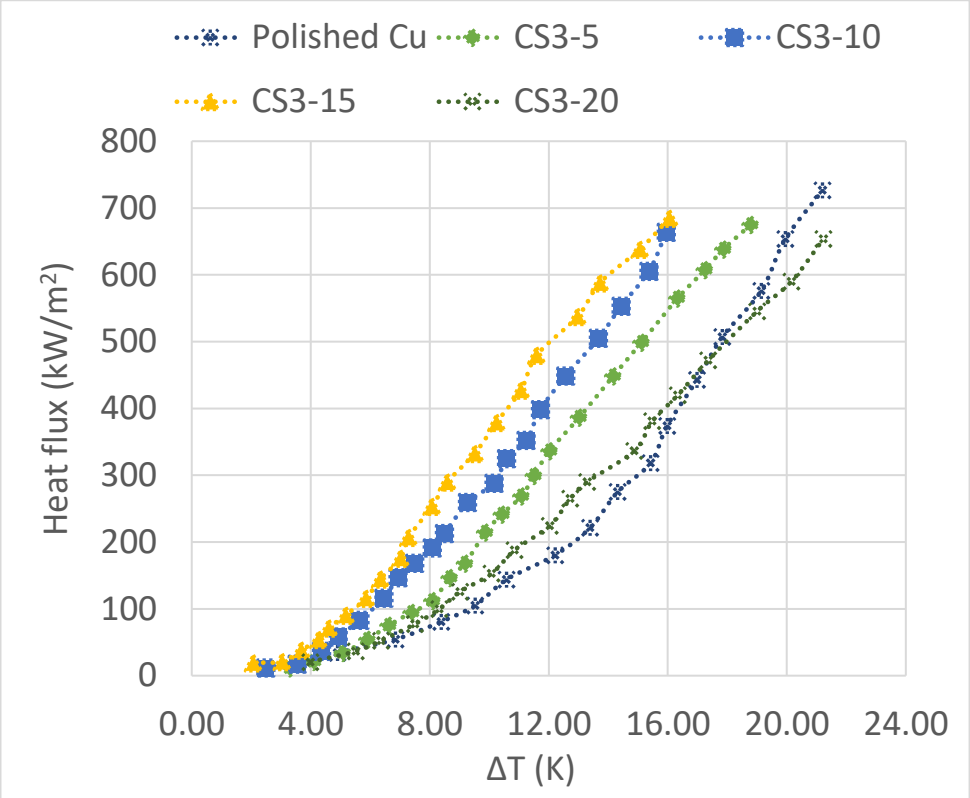

Fig. 5.3. Pool boiling performance curve of SiO_2 - Al_2O_3 coated surfaces.

In the case of composite texture CS3-5, CS3-10, and CS3-15 also, a significant reduction in wall superheat observed, this may be because of the decrease in wettability. On the contrary to this for the surface CS3-20, despite considerable decrees in wettability there was considerably higher wall superheat observed, which indicates wettability effect in wall superheat reduction is limited for a certain coating layer thickness. In the present case, the decrease in surface wettability was found to be effective for reduction in wall superheat only when coating layer thickness was below ~27µm. Apart from low wettability, other parameters such as roughness and texture of the surface also were collectively responsible for significant reduction in wall temperature. However, beyond the optimum coating layer thickness,

increased thermal resistance plays a vital role in poor heat dissipation and considerably higher wall temperature, which is observed for the sample CS3-20, where coating layer thickness is ~35µm.

5.2. Effects on ONB temperature

The onset of nucleate boiling (ONB) is a critical factor in the cooling of electronic devices. The temperature at which bubbles start to form on the wall, known as ONB, which have special significance. Any delay in ONB can lead to a sudden temperature spike, potentially causing the device towards thermal damage. Therefore, lowering the ONB temperature can help shield the device from thermal shock. Figure 5.4, shows the ONB point on TiO_2-SiO_2 coated surfaces with round circles. As the figures indicate the wall superheat at ONB initially decreases with the increase in coating duration and then increases. The ONB for coated surfaces CS1-5, CS1-10, CS1-15, and CS1-20, respectively are 7.6, 6.3, 5.9, and 8 K, whereas for polished Cu surface is 9.5 K. Figure 5.5 Shows the wall superheat at ONB for polished Cu surface and all coated surfaces.

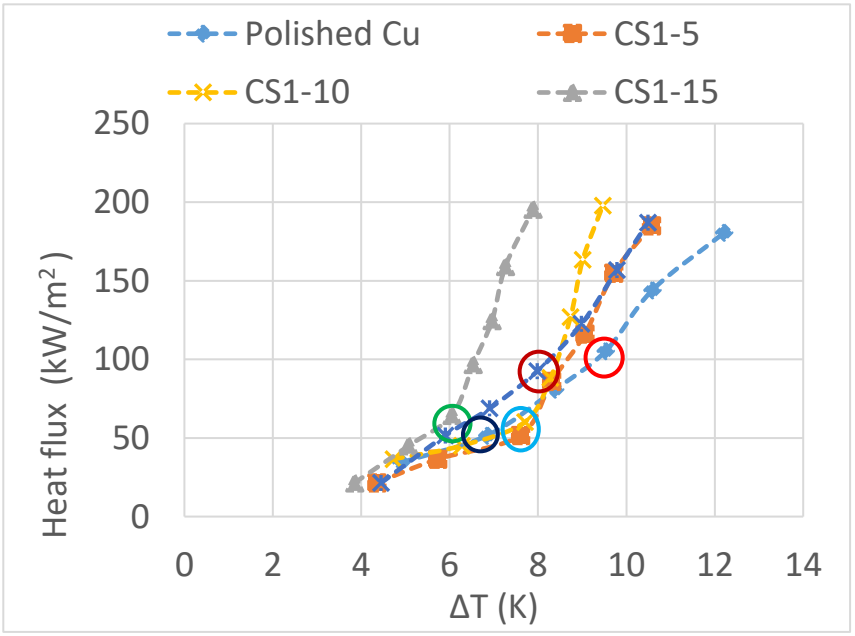

Fig. 5.4. ONB points marked with the circle on the boiling curve of TiO_2-SiO_2 coated samples.

The largest reduction in ONB was observed for the sample CS1-15, which is nearly 38 % lower than the polished Cu surface. Similarly, for TiO_2 - Al_2O_3, and SiO_2 - Al_2O_3 coatings the largest reduction in ONB are 5.5 K and 6.5 K, respectively for the sample CS2-10, and CS3-15, which are nearly 58% and 68% lower than the on bare surface.

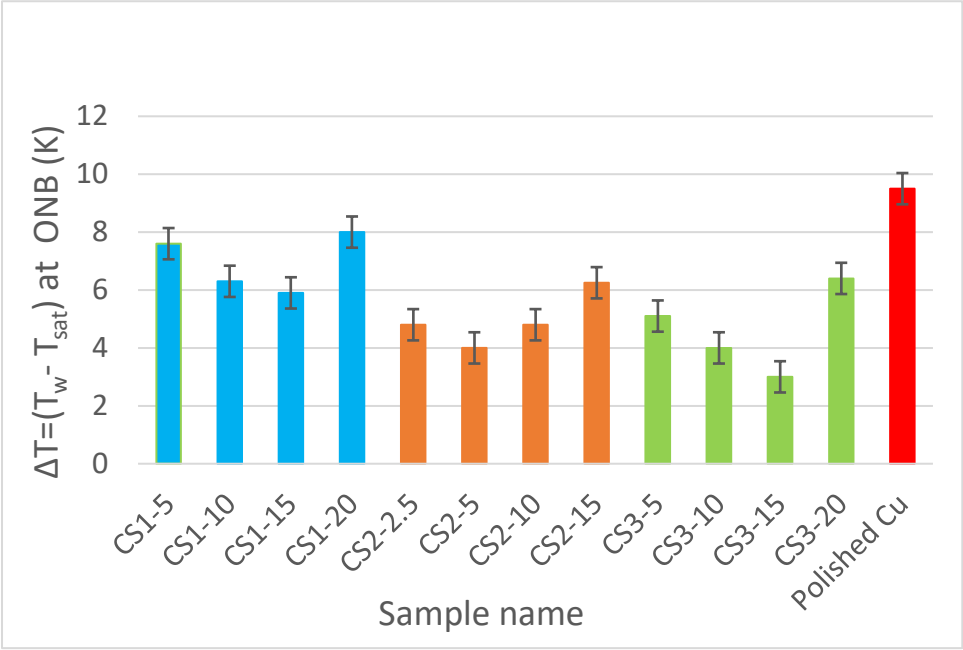

Fig. 5.5. Comparison of wall superheat temperature when bubble formation initiated on the surface.

Based on the experimental results it can be stated that compared to hydrophilic surface ONB relatively occurs at lower wall temperatures on hydrophobic surfaces. Similar observations were also reported in the study conducted by Mohammadi et al. [127] recently and Bourdon et al. [111] in the past. The early ONB is a particular feature of hydrophobic surfaces that can be used to prevent thermal damage to highly temperature-sensitive surfaces such as sensors and electronic chips [85]. The reduction in ONB temperature of hydrophobic surfaces can be attributed to significant changes in surface wettability and textured of coated surfaces. It has already been shown in Chapter 3 (Section 3.2.1.1) that, on the surface of CS1-10 and CS1-15

a large number of micro/nanovoids and cone shape cavities, were present, which act as active nucleation sites during the boiling process.

Qualitatively, the size (mouth diameter) of cone-shaped cavities (Fig. 3.8c) is relatively larger than the voids (Fig. 3.8b). Kumar et al. [85] have described in their study that ONB is a general function of nucleation sites and micro-sizes cavities. Also, large cavities activate at lower wall temperature on the hydrophobic surface which is responsible for the early ONB [83]. The influence of cavity size was also observed in the present study, where smaller micro/nanovoids (CS1-10) showed less reduction in ONB compared to the larger cavities (CS1-15). A minor reduction in ONB on CS1-5 shows the influence of wettability rather than the nucleation sites. Contrary to these a minor reduction in ONB was observed for the surface CS1-20, this may be because of comparatively higher coating thickness which suppressed the wettability effects and increased the thermal resistance of the surface, which caused a delay in the ONB. Another observation is that the size of the crack is smaller and in the nano range with respect to the CS1-10 and CS1-15 which is also responsible for delay in ONB because smaller cavities required higher wall superheat to active and act as nucleation sites. This can be easily correlated with the classical theory for hydrophobic surfaces (Eq. 5.1) [86], which gives the correlation of minimum wall superheat requirement for bubble initiation and growth for a known cavity radius.

$$\Delta T > \frac{2\sigma T_{sat} v_{lv}}{(h_{lv}\, \mathrm{r})} \tag{5.1}$$

In the above equation, σ denotes the liquid surface tension, T_{sat} is liquid saturation temperature, v_{lv} is specific volume between the saturated vapour and liquid and r is the cavity radius. Similarly, for TiO_2 - Al_2O_3, coated surface, CS2-5 has a greater number of micro/nano cavities in the form of dimples (Fig. 3.9b) which is responsible for the maximum ~58% reduction in ONB. For the case of SiO_2 - Al_2O_3 coating, wettability decreases as coating duration increases. With decrees in wettability, ONB temperature also decreases and a maximum 68% reduction

is observed for the 15 minutes coated surface (CS3-15). The significant reduction in wettability plays a key role in the early ONB and low wall temperature. For the sample CS3-20, significantly higher coating thickness suppresses the wettability effect and delays the ONB due to increased thermal resistance.

5.3. Effects on heat transfer coefficient

The boiling heat transfer coefficient (BHTC) is an important parameter by which the performance of a device is measured. In the present study, the BHTC of all surfaces is calculated using Eq. 5.2, which represents the slope of the supplied heat flux on the boiling curve as a function of wall superheat (ΔT).

$$h = \frac{q^{"}}{(T_w - T_l)} \tag{5.2}$$

5.3.1. Effect of TiO_2-SiO_2 coating

Figure 5.6 shows the results of the heat transfer coefficient of polished Cu and TiO_2-SiO_2 coated surfaces in Milli-Q water. The results showed that when applied heat flux increases, the HTC also increases. Because with an increase in applied heat fluxes, surface temperature also increases, which decreases the adhesion energy (surface tension) between the surface and liquid [128]. Due to decreases in adhesion energy bubbles from the smaller cavities also gets active, resultant nucleation density increase, and, subsequently HTC increases. With reference to the Mikic and Rohsenow correlation [128] (Eq. 5.3), nucleation site density plays a key role in HTC enhancement.

$$HTC = 2(\pi K_l \rho_l C_{pl})^{0.5}\, n_a (D_b)^2 (f_b)^{0.5} \tag{5.3}$$

Another important observation is samples CS1-5, CS1-10, and CS1-15 exhibit a steeper slope, relative to the bare surface, particularly below the heat flux of 400 kW/m^2. Beyond this point, a rapid decrease in HTC is observed for CS1-5, while it continues to

increase for CS1-10 and CS1-15. The maximum enhancements in HTC for CS1-5, CS1-10, and CS1-15 are 23.5%, 38%, and 62%, respectively. The heat flux corresponding to the maximum HTC are 330 kW/m^2, 275 kW/m^2, and 230 kW/m^2.

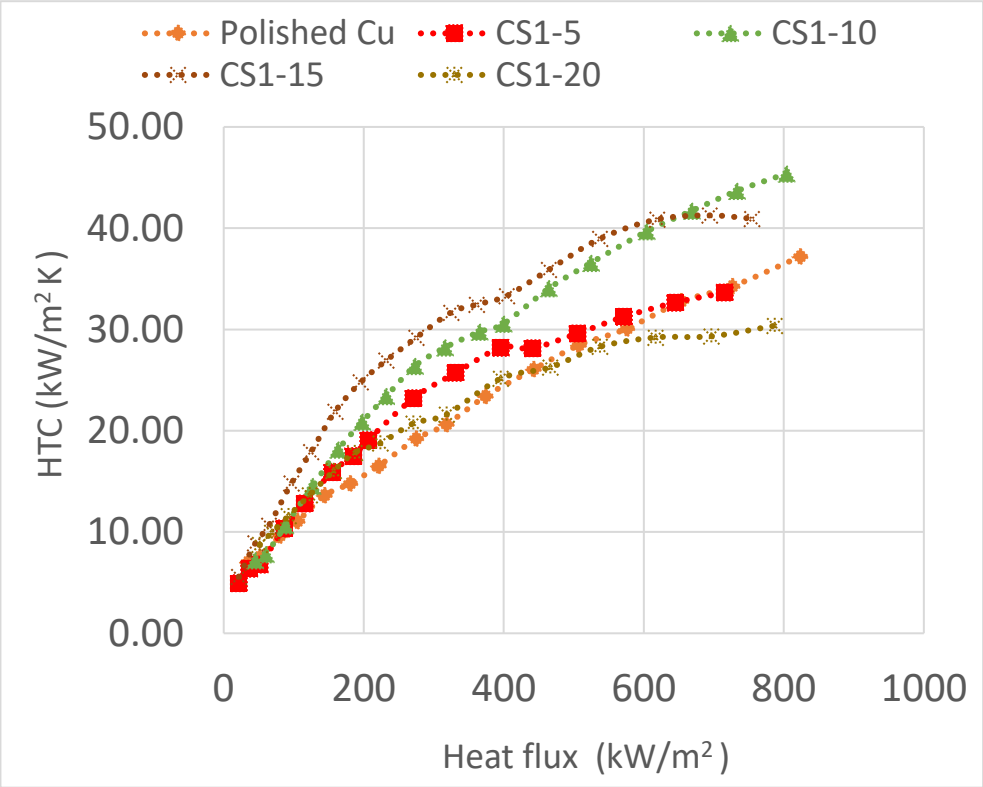

Fig. 5.6. Plot of heat transfer coefficient against the heat flux of TiO_2-SiO_2 coated and Polished Cu surfaces.

Figure 5.7 shows the percentage enhancement in HTC against the applied heat fluxes. Results indicate that, initially HTC increases with the applied heat flux, reaches its maximum, and then starts degrading. The HTC enhancement in the low heat flux region ($q'' < 400$ kW/m^2) is more significant than the higher heat flux, except for sample CS1-20. A separate bar diagram has been drawn to show the influence of the composite coating on maximum enhancement in HTC and same has shown in Fig. 5.8. From Fig. 5.8 it is clear that the maximum and minimum enhancement in HTC is 62% and 18% for the sample CS1-15 and CS1-20, respectively. As the coating duration increases heat flux value corresponding to the maximum enhancement decreases.

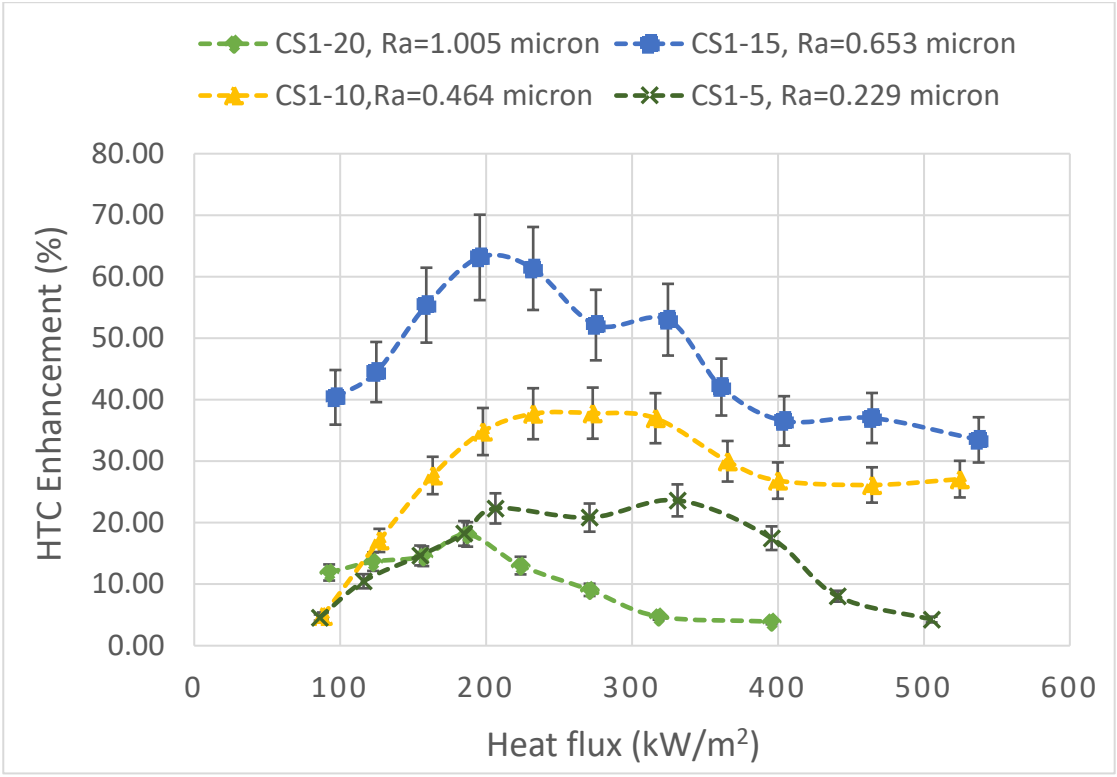

Fig. 5.7. Variation in HTC enhancement at different heat flux onTiO_2-SiO_2 coated samples.

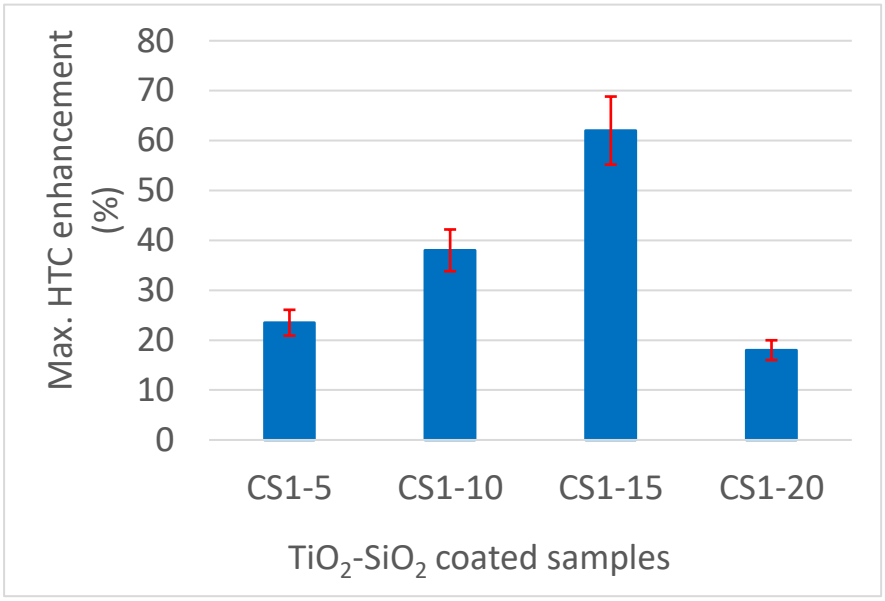

Fig. 5.8. Plot of maximum enhancement in heat transfer coefficient (HTC) of TiO_2-SiO_2 coated samples.

The variations in HTC enhancement can be attributed to the roughness and surface texture of the surfaces. The roughness of the sample CS1-5 appears relatively close to the polished Cu, whereas samples CS1-10 CS1-15, and CS1-20 have considerably higher roughness (R_a). Also, surface CS1-10 and CS1-15, respectively have many voids and cone-shaped cavities which act as artificial nucleation sites on the surface. It has already been discussed that qualitatively, the size (mouth diameter) of cone-shaped cavities (Fig. 3.8c) is relatively larger than the voids (Fig. 3.8b). Yao et al. [83] stated that the large cavity required comparatively less wall superheat temperature to activate and form bubbles. Therefore, at similar heat flux conditions initially, more bubbles are generated on the larger cavity surface (Refer chapter 6 for bubble visualization), due to which vapour generation rate increases and wall superheat temperature decreases, Consequently, the slope of the boiling curve is higher, which is nothing but HTC is higher. This is the reason why maximum enhancement was observed at comparatively low heat flux on sample CS1-15.

Since bubble sizes also depend on the cavity size [83, 129], comparatively bigger bubbles may have been generated on the surface of CS1-15 (Refer chapter 6 for bubble visualisation snap shot), which coalesce earlier than the smaller bubbles. Once the bubble starts coalescing, departure frequency decreases and wall superheat starts increasing at a higher rate, which became a cause for the HTC deterioration. As the heat flux keeps on increasing deterioration in HTC is also increasing, and its effects are more prominent at higher heat fluxes. That's the reason behind lower HTC on CS1-15, than on CS1-10 beyond the heat flux ~600 kW/m^2. For the sample CS1-5, which has a relatively smoother surface that produced small and less active nucleation sites, due to which improvement in HTC is considerably less.

The sample CS1-20 shows poor HTC performance among the coated surfaces studied here. If only the roughness factor was considered, it could have provided maximum HTC at the initial

stage, because it has the highest roughness among all the surfaces. But, in this case, higher coating thickness is one of the primary reasons behind heat transfer deterioration and relatively higher ONB. Since, there were delays in ONB, causes vapour generation rate was reduced, subsequently wall superheat temperature increased and HTC decreased.

5.3.2. Effect of TiO_2-Al_2O_3 coating

Figure 5.9 illustrates how the experimental heat transfer coefficient varies with the heat flux for both bare and coated surfaces. For all surfaces, as the heat flux increases, HTC also increases. The increase in HTC is more noticeable at low heat fluxes, while at higher heat fluxes, the rate of increase in HTC decreases for all surfaces. Sample CS2-5 outperforms all other samples in terms of the HTC enhancement, while CS2-15 performs the worst. Initially, CS2-15's performance was similar to that of the bare surface, but as the heat flux exceeded 250 kW/m², its performance deteriorated and became even worse than that of the polished Cu at higher heat fluxes.

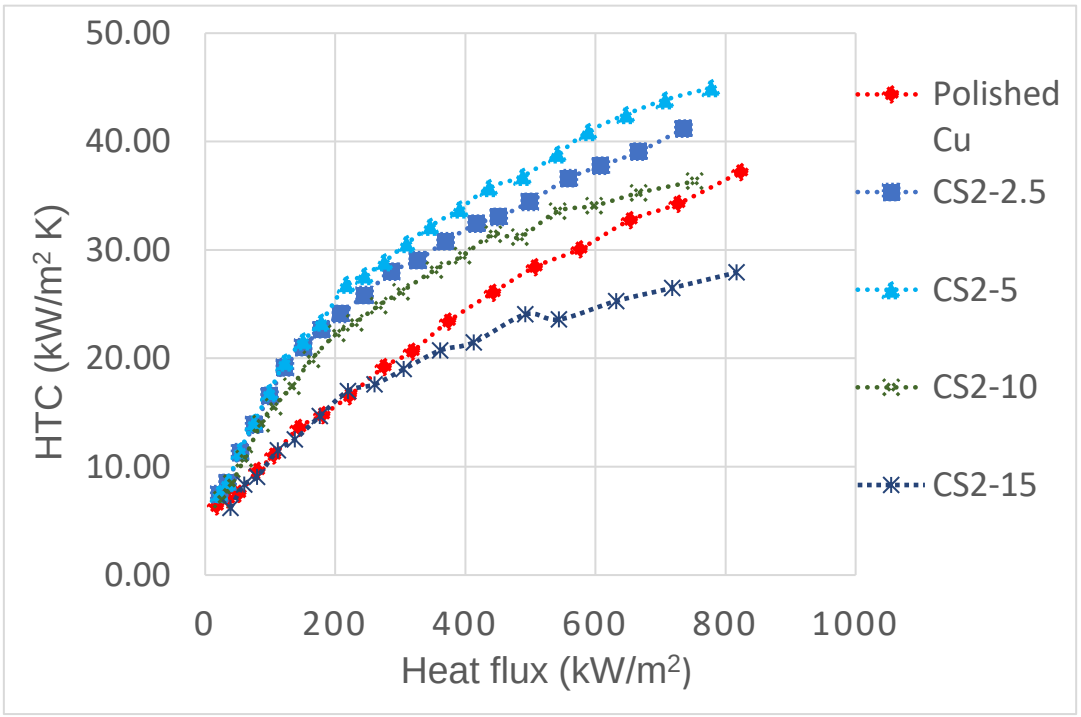

Fig. 5.9. Plot of experimental heat transfer coefficient against the heat flux of TiO_2-Al_2O_3 coated and Polished Cu surfaces.

The maximum HTCs for the samples CS2-2.5, CS2-5, CS2-10, CS2-15, and polished Cu are 41.2, 44.96, 36.3, 27.91, and 37.2 kW/m²-K, respectively.

For a better understanding, the percentage change in HTC with reference to the bare surface has been calculated and a curve has been plotted against the heat flux as shown in Fig. 5.10. Notably, for sample CS2-15, the enhancement is negative, which indicates poorer performance than the bare (polished) surface. Figure 5.11 gives a clearer picture of maximum enhancement of HTC, for all textured surfaces. The maximum enhancements in HTC observed for CS2-2.5, CS2-5, and CS2-10, are 50, 63, and 43 %, respectively, while for CS2-15 it is only 4 %. The rate of enhancement was more prominent in the low heat flux regime because on a hydrophobic surface, bubbles start generating comparatively a low wall superheat temperature [111-127].

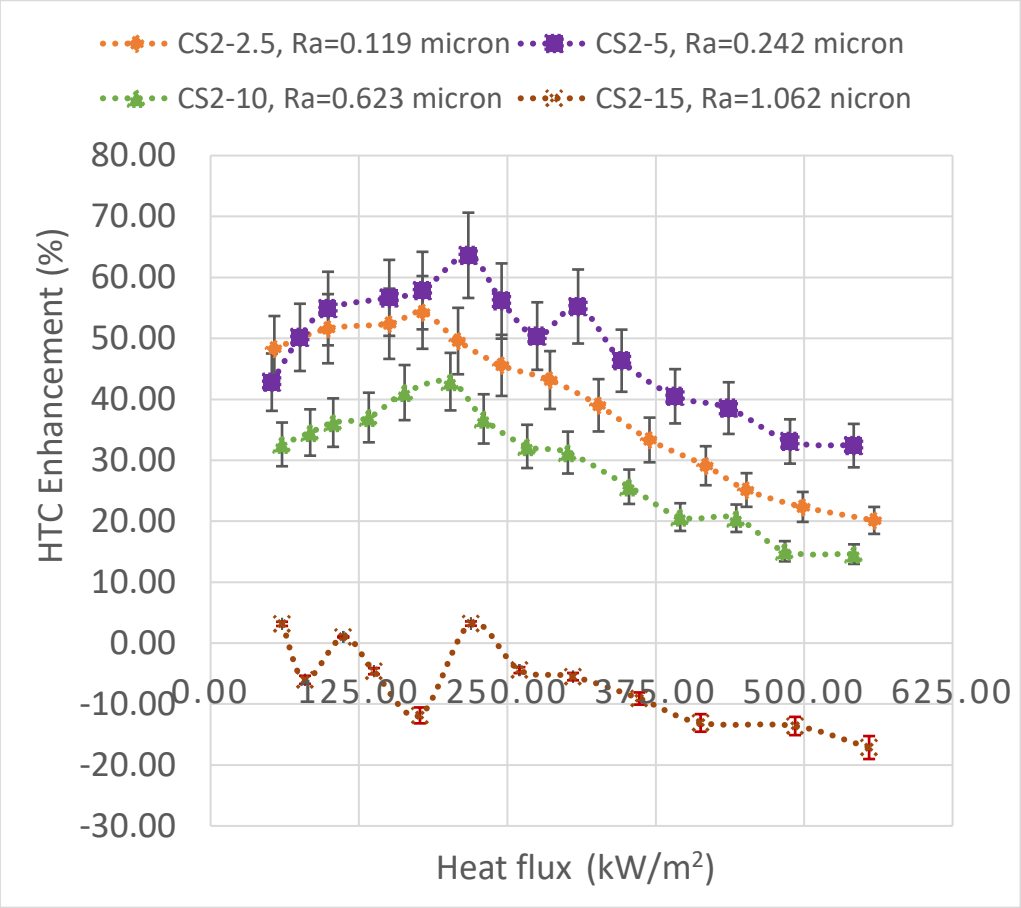

Fig. 5.10. Illustration of HTC enhancement on TiO_2-Al_2O_3 coated samples against the supplied heat fluxes.

Similar to the previous case (TiO_2-SiO_2 coatings) the higher nucleation sites and bubble frequencies play a significant role in higher HTC, particularly below the 250 kW/m^2. In Chapter 6 of this thesis, effects of surface wettability on bubble dynamic have also discussed.

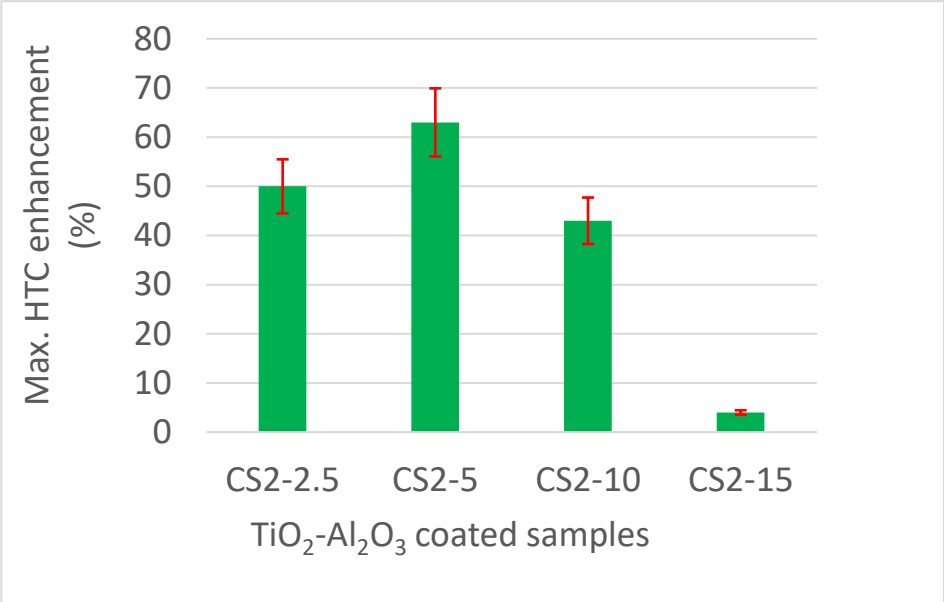

Fig. 5.11. Illustration of Max. Enhancement in heat transfer coefficient (HTC) on TiO_2-Al_2O_3 coated samples.

However, in a similar study, Jo et al. [130] reported that in the case of a hydrophilic surface, bubbles leave the surface smoothly, whereas on a hydrophobic surface, they elongate and form a necking pattern then divide into two parts; one departs and the other remains on the surface, which grows further and forms another bubble on the surface much earlier than on a hydrophilic surface (Detailed study of bubble dynamics presented in Chapter 6). With this approach, a chain of bubbles forms on the surface without any delay in the bubble generation waiting period, consequently, bubble departure frequency increases. From the above discussion, we can say that, in low heat flux region, higher nucleation sites and increased bubble frequency lead to a higher HTC, while increased departure diameter and bubble frequency are key factors for maintaining a higher HTC even at higher heat flux for CS2-2.5 and CS2-5. For sample CS2-10 HTC was initially increased and later when applied

heat flux reached beyond~540 kW/m^2 it starts deteriorating rapidly. On the Contrary to these, on sample CS2-15 enhancement in HTC is negligible at low heat flux region ($q'' < 250$ kW/m^2), and beyond it worse than the Polished Cu. This happen because considerably higher coating thicknesses act as an insulating layer due to which thermal resistance increased, and consequently HTC decreased even below the polished Cu as noticed for the sample CS2-15.

5.3.3. Effect of SiO_2 - Al_2O_3 coatings

The experimental heat transfer coefficient of SiO_2 - Al_2O_3 coated samples and Polished Cu has evaluated as given by Eq. 5.2, and presented in Fig. 5.12. It depicts HTC variation with the supplied heat flux. Experimental results show that compared to the polished Cu surface, the coated samples CS3-5, CS3-10, and CS3-15 have higher HTC, whereas for the case of sample CS3-20, it was initially marginally increased and later performance decreased to below the polished Cu. It is also observed that the HTC continuously increases with the supplied heat flux. However, the increment rate at all heat fluxes is not similar.

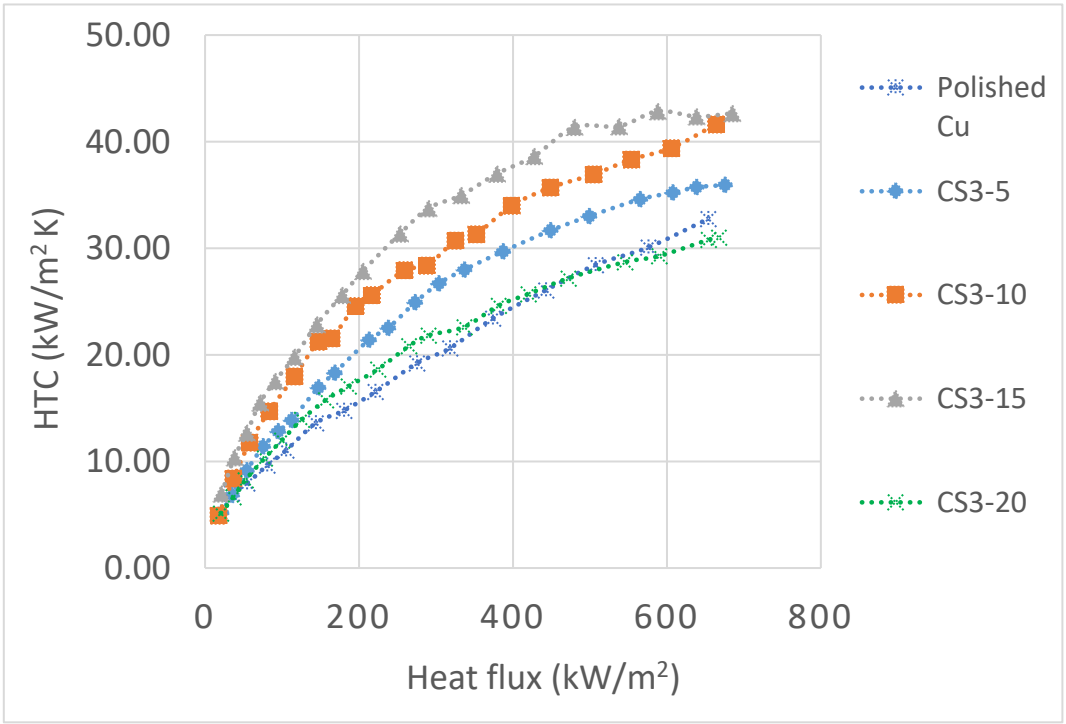

Fig. 5.12. Variation of experimental heat transfer coefficient against the heat flux of SiO_2-Al_2O_3 coated and Polished Cu surfaces.

Initially, enhancement in HTC increases with the heat flux, reaches a maximum, and then starts to decrease. Qualitatively, the enhancement in the low heat flux region ($q'' < 350$ kW/m^2) is more significant than the higher heat fluxes ($q'' > 350$ kW/m^2) as shown in Fig. 5.13. In comparison to the polished Cu, the greatest and lowest enhancement in HTC was observed for the CS3-15 and CS3-20, respectively. The maximum enhancement in HTC on CS3-5, CS3-10, CS3-15, and CS3-20 are nearly 34%, 59%, 75%, and 14%, corresponding to the heat flux 304, 217, 178, and 157 kW/m^2 respectively as shown in Fig. 5.14. Significant increases in HTC can be attributed to change in wettability and roughness of the samples after the coating.

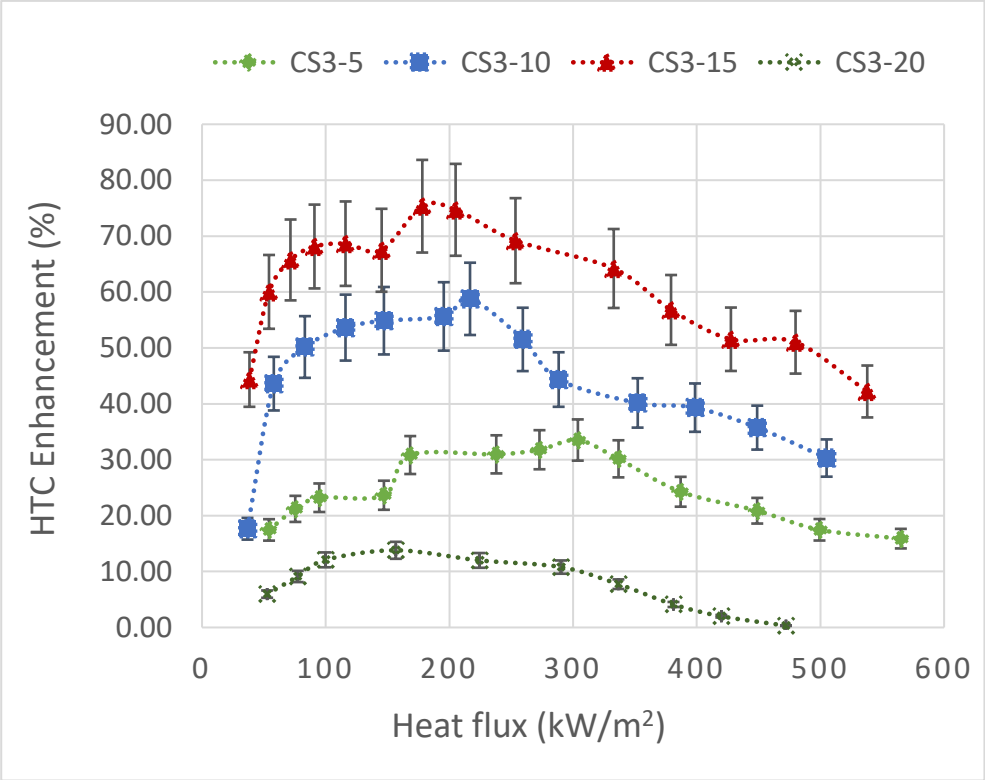

Fig. 5.13. Variation in HTC enhancement at different heat flux on SiO_2-Al_2O_3 coated samples.

It has already been discussed (Chapter 3) that all coated surfaces are hydrophobic in nature while polished Cu is hydrophilic in nature. Based on the experimental results on the first three samples HTC is significantly higher than the polished Cu one, whereas on the fourth sample CS3-20, it first increases marginally and then showed poor than the polished Cu. The higher

HTC on hydrophobic surfaces is consistent with the other studies conducted on similar wettability surfaces in various literature [57, 75, 129]. It is stated that the bubble nucleation on a hydrophobic surface starts at low wall superheat and generates more bubbles at similar heat fluxes. Since vapour generation extracts extra heat in the form of latent heat of vaporization causes wall superheat temperature to decrease, subsequently heat transfer coefficient increases.

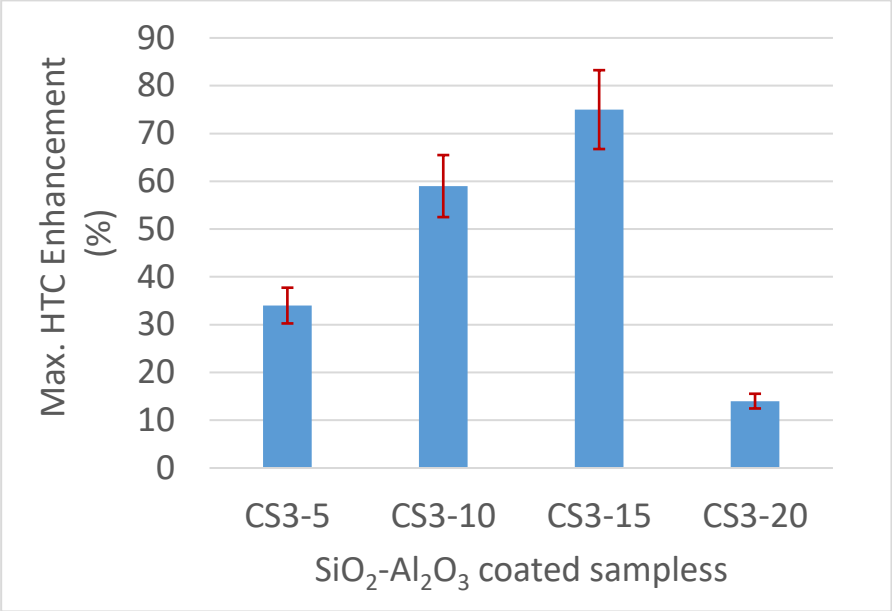

Fig. 5.14. Plot of maximum enhancement in heat transfer coefficients (HTC) on SiO_2-Al_2O_3 coated samples.

Bubble generation at low wall superheat on a hydrophobic surface can also explained by thermodynamic consideration of bubble nucleation theory [129]. Eq. (5.4) known as Young –Laplace correlation which correlates the vapour pressure, liquid pressure, and the radius of curvature of a vapour bubble on a solid surface. On a hydrophobic surface (Fig. 5.15a) curvature radius on an embryonic bubble is negative.

$$\Delta P = Pv - P_l = \frac{2\sigma}{r} \tag{5.4}$$

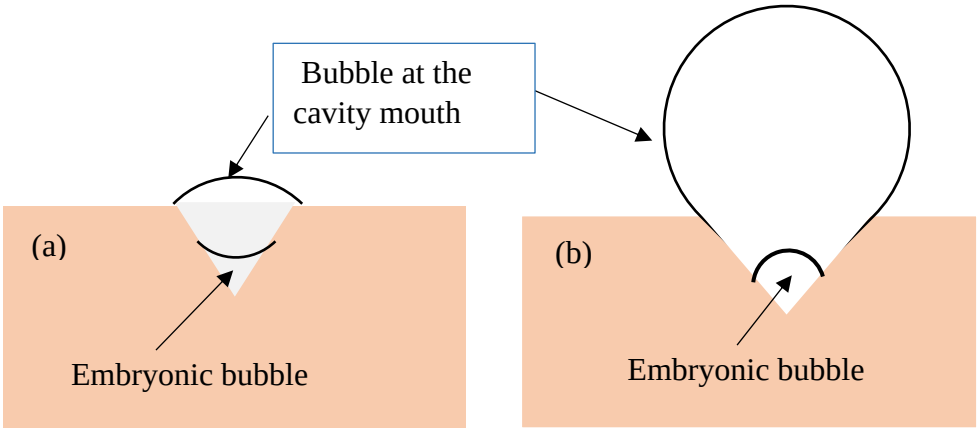

Fig. 5.15. Illustration of liquid-vapour interface at the (a) Hydrophobic surface (b) Hydrophilic surface [129].

According to Eq. (5.4), to correctly hold the equation, ΔP should be negative which is possible only when the liquid pressure is greater than the vapour pressure. It means Tsat (P_v) is lower than the T_l, as a result, the embryonic bubble in the cavity is covered by the superheated liquid, which has the capacity to grow even at low wall superheat (ΔT) and low heat flux. An additional heat supplied can accelerate the bubble growth and frequency of a bubble. Contrary to this, on a hydrophilic surface (Fig. 5.15b) the radius of curvature of an embryonic bubble in the cavity is positive. It means vapour pressure is higher than the surrounding liquid pressure, and Tsat (P_v) is higher than the surrounding liquid saturation temperature at atmospheric pressure. So, to generate a bubble additional heat is required to evaporate the surrounding liquid at the liquid-vapour interface.

Figure 5.15 also demonstrates the radius of curvature of vapour bubbles on a hydrophobic and hydrophilic surface outside the cavity. Qualitatively, the radius of bubble curvature on a hydrophobic surface is larger than that on a hydrophilic one. From Eq. (5.1) it is clear that a low wall superheat is needed to grow the bubble on a hydrophobic surface, as a result, HTC is higher.

5.4. Wettability and roughness effects

The surface wettability of all the surfaces has been evaluated by contact angle measurements. discussed in chapter 3. Contact angle measurements showed that all coated surfaces are hydrophobic by nature while polished Cu is hydrophilic by nature (see section 3.2.5). A hydrophilic surface can spread the water over a large surface region. In contrast, on a hydrophobic surface fluid formed a compact droplet and minimized the contact area on the surface. It implies that the wettability of the coated (hydrophobic) surfaces is relatively less than that of the polished Cu (hydrophilic surface).

The surface roughness (R_a) of all the samples was analysed by surface profilometer and the result is presented in Chapter 3. It has been found that the surface roughness of coated surfaces is greater than the polished Cu surface, and R_a increases as coating duration increases. The highest R_a observed for CS1-20, CS2-15, and CS3-20, respectively for the TiO_2-SiO_2, TiO_2 - Al_2O_3, and SiO_2 - Al_2O_3 coatings.

Since boiling is associated with the interaction between solid and liquid [16], surface roughness [125, 129], and wettability [18,117, 127] play a very crucial role in the boiling heat transfer phenomenon. However, both parameters are related to each other and can't be ignored either of these completely.

The effect of surface wettability and nucleation rate ($\dot{n}$) in terms of contact angle can also be understood by an expression proposed by Cole [131], which can be expressed as:

$$\Delta T = \frac{T_{sat}}{\rho_v h_{lv}} \left[\frac{16\pi\sigma^3 f(\theta)}{3kT_l \, ln\left({\dot{n}T_l}/{h_c}\right)} \right]^{0.5} \tag{5.5}$$

In the above expression σ is the surface tension of liquids; k is the Boltzmann constant; h_c is the Planck constant; $\dot{n}$ is the rate of nucleation; and f(θ) is a free energy related function, which depends on contact angle (θ) as follows:

$$f(\theta) = \frac{2+3\cos\theta-(\cos\theta)^3}{4} \quad (5.6)$$

The function *f(θ)* decreases as contact angle (θ) increases, and its effect is insignificant when contact angle is less than 30° or greater than 150° as shown in Fig. 5.16. From Eq. (5.5), and (5.6), it can be understood that the changes in wall superheat temperature depends on the contact angle and nucleation rate of the surfaces for a particular liquid.

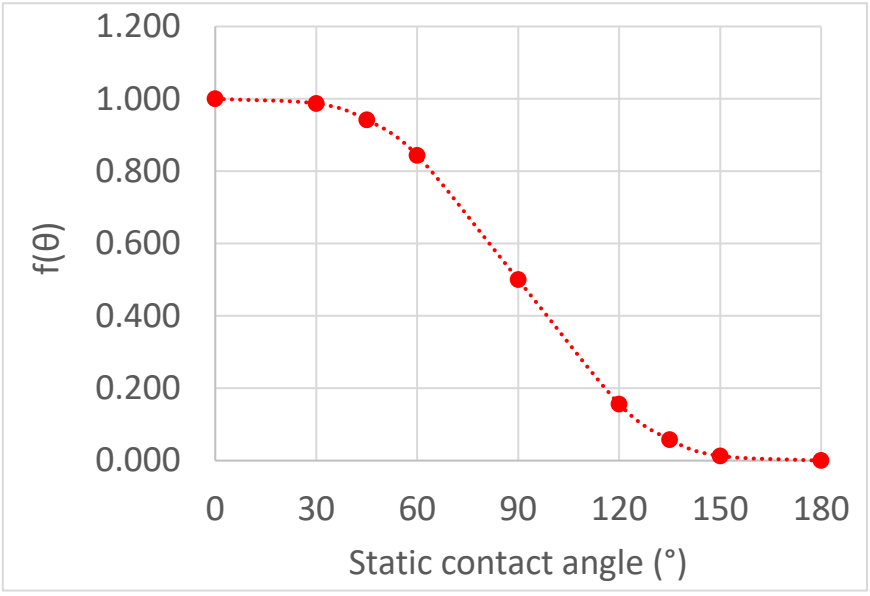

Fig.5.16. Plot of free energy related function f(θ) against the contact angle (θ).

Since the roughness effect always exists along with the wettability effect, therefore it is not possible to completely eliminate either of these two in experimental investigations [111]. Even though contact angles are higher on surfaces CS1-5 and CS1-10, but reduction in ΔT is largest on CS1-15 particularly below the region of heat flux 600 kW/m^2. Because surface roughness (R_a) considerably higher than CS1-5 and CS1-10, due to which nucleation rate considerably higher, which plays a key role in early bubble formation and higher reduction in wall superheat (ΔT). Similarly, for the CS2-10, a higher R_a responsible for early bubble formation and higher nucleation sites, resultant wall superheat reduced and HTC increased.

5.5. Effects of coating thickness

In the present study, the effects of coating layer thickness on boiling heat transfer have been interpreted based on the experimental outcomes after the implementation of it on three different groups of binary oxide coatings. Experiments were performed on different samples whose coating layer thicknesses were different. It has already been discussed in Chapter 3 that in all three cases, coating layer thickness increases with the increasing coating duration. It implies that the surface coated for a higher coating duration has a higher coating layer thickness. In all three groups of coatings, it has been observed that the surface roughness and surface wettability also varied with the coating duration. Since, control over surface topography, morphology, and wettability has not been made while varying the coating thickness. Hence, the role of the coating layer in favour of BHTC enhancement can't studied explicitly. However, based on the experimental results it can't be denied that if the coating layer thickness crosses a range it becomes a cause for the BHTC deterioration. When the coating layer thickness crosses the critical limit, it starts acting as an insulating layer due to which heat transfer is affected. However, the critical layer of coating thickness varies for all the three cases (TiO_2-SiO_2, TiO_2 - Al_2O_3, and SiO_2 - Al_2O_3 coatings) studied here. Its value depends on many factors such as materials type (metals, metal oxides, or composites), kind of structure formation (porous or non-porous), etc.

The pool boiling performance characteristics (Boiling curve and HTC performance) of all three groups of coatings have been discussed in details of sections 5.2 and 5.3. The pool boiling performance results show that in the case of TiO_2-SiO_2 coating up to ~10µm layer of thickness, BHTC was improved. When the coating layer of a sample (CS1-20) further increased to 14.58µm its performance declined and went down below the polished Cu at higher heat fluxes ($q'' > 460$ kW/m^2). Similarly, for the other two cases, the experimental optimum layer of thicknesses are ~15µm and ~27µm observed on TiO_2-Al_2O_3 (CS2-5), and SiO_2-Al_2O_3 (CS3-

20), coatings, which indicates there is an optimum layer of thickness exist up to that boiling performance not get affected, and beyond it, start affecting the boiling performances adversely.

At this point, someone may have questioned how did you interpreted that, the coating layer thickness is responsible for the BHTC deterioration. The simple reason is that the higher surface roughness and reduced wettability of sample CS1-20, show a favourable condition for BHTC enhancement, but experimental results showed significant deterioration in it, therefore the higher coating layer thickness of sample CS1-20 is the only reason that increased the thermal resistance of a surface, resultant fall in BHTC observed. Also, its effect increases as the supplied heat flux increases. As discussed, two more cases (TiO_2-Al_2O_3, and SiO_2-Al_2O_3) have been considered and experiments were performed to confirm the assumption. In both cases, an optimum range of coating layer thickness also existed up to that BHTC was increased and beyond it deteriorated. A Summarized result of optimum coating layer thickness and corresponding surface properties as well as BHTC enhancement is presented in Table 5.1. as below.

Table 5.1. Summarized result of optimum coating layer thickness and corresponding surface properties as well as BHTC enhancement.

Type of coatings	**Optimum coating layer thickness (µm)**	**Surface roughness (µm)**	**Sessile drop Contact angle**	BHTC enhancement (%)
TiO_2-SiO_2 coating	10	0.464	100.3°	62
TiO_2-Al_2O_3 coating	15	0.242	100°	63
SiO_2-Al_2O_3 coating	27	0.880	120.1°	75

5.6. Summary

In this chapter results of pool boiling performance of different binary oxides coating and the effects of textured, wettability, roughness, and coating layer thickness has discussed. Three different types of binary composites textured (TiO_2- SiO_2, TiO2-Al_2O_3, and SiO_2-Al_2O_3) have been studied. In each case, four different surfaces were analysed which have different wettability, roughness, and coating layer thickness. Experimental results indicate that boiling heat transfer performances of coated surfaces increased if coating thickness was kept below an optimum range. The optimum range implies that if a surface has been coated and thickness kept near the optimum range, boiling heat transfer will have the greatest enhancement due to texturing, wettability, and roughness effects. If the coating layer thickness is kept higher than the optimum range, the performance of BHTC will degrade, causing surface temperature will increase and, in some cases, thermal damage may occur due to a sudden jump in temperature. The optimum coating layer thickness for the case of TiO_2-SiO_2, TiO_2-Al_2O_3, and SiO_2-Al_2O_3 are ~10µm, ~16µm, and ~27 µm, respectively. The maximum enhancement in BHTC for the corresponding cases is 62%, 63%, and 75% respectively.

****

**********This page intentionally left blank**********